Research Article

Rapid Communications in Mass Spectrometry

Received: 8 June 2015 Revised: 14 September 2015 Accepted: 18 September 2015 Published online in Wiley Online Library

Rapid Commun. Mass Spectrom. **2015**, *29*, 2385–2401
(wileyonlinelibrary.com) DOI: 10.1002/rcm.7400

An ultrahigh-resolution mass spectrometry index to estimate natural organic matter lability

Juliana D'Andrilli[1,2*], William T. Cooper[3], Christine M. Foreman[1,2] and Alan G. Marshall[3,4]

[1]Department of Chemical and Biological Engineering, Montana State University, Bozeman, MT 59717, USA
[2]Center for Biofilm Engineering, Montana State University, Bozeman, MT 59717, USA
[3]Department of Chemistry & Biochemistry, Florida State University, Tallahassee, FL 32306, USA
[4]Ion Cyclotron Resonance Program, National High Magnetic Field Laboratory, Florida State University, Tallahassee, FL 32310, USA

RATIONALE: Determining the chemical constituents of natural organic matter (NOM) by Fourier Transform Ion Cyclotron Resonance Mass Spectrometry (FTICRMS) remains the ultimate measure for probing its source material, evolution, and transport; however, lability and the fate of organic matter (OM) in the environment remain controversial. FTICRMS-derived elemental compositions are presented in this study to validate a new interpretative method to determine the extent of NOM lability from various environments.
METHODS: FTICRMS data collected over the last decade from the same 9.4 tesla instrument using negative electrospray ionization at the National High Magnetic Field Laboratory in Tallahassee, Florida, was used to validate the application of a NOM lability index. Solid-phase extraction cartridges were used to isolate the NOM prior to FTICRMS; mass spectral peaks were calibrated internally by commonly identified NOM homologous series, and molecular formulae were determined for NOM composition and lability analysis.
RESULTS: A molecular lability boundary (MLB) was developed from the FTICRMS molecular data, visualized from van Krevelen diagrams, dividing the data into more and less labile constituents. NOM constituents above the MLB at H/C $\geq$1.5 correspond to more labile material, whereas NOM constituents below the MLB, H/C <1.5, exhibit less labile, more recalcitrant character. Of all marine, freshwater, and glacial environments considered for this study, glacial ecosystems were calculated to contain the most labile OM.
CONCLUSIONS: The MLB extends our interpretation of FTICRMS NOM molecular data to include a metric of lability, and generally ranked the OM environments from most to least labile as glacial > marine > freshwater. Applying the MLB is useful not only for individual NOM FTICRMS studies, but also provides a lability threshold to compare and contrast molecular data with other FTICRMS instruments that survey NOM from around the world. © 2015 The Authors. *Rapid Communications in Mass Spectrometry* published by John Wiley & Sons Ltd.

Natural organic matter (NOM) is a significant component of marine, freshwater, and glacial ecosystems, affecting multiple biogeochemical processes in the environment.[1–7] The combination of allochthonous and autochthonous inputs in aquatic ecosystems contribute greatly to the chemical complexity of organic matter (OM), including an assortment of biochemically identifiable compound classes.[8,9] Microorganisms utilize and produce autochthonous OM during microbial metabolism, a relationship that links the microbes to the quality and quantity of OM.[10] OM quality is determined by the mixture of different types of chemical species, including labile and recalcitrant compounds. Therefore, the OM quality/chemical character is important to investigate, as it plays a role in microbial metabolism and carbon turnover rates. Within ecosystems, OM is introduced and/or produced, transformed, stored, and transported to downstream ecosystems; yet its origin, chemical characteristics, and overall contribution to the global carbon cycle are not well defined.

Determining the molecular composition and fate of OM in aquatic environments is essential to better understand the global carbon cycle.[10–12] Until recently, the ability to identify OM components, sources, and chemical processes was very limited. However, determining the chemical constituents of OM at the molecular level remains the ultimate measure for probing OM source material, evolution, and transport, and is used to trace lipid-, protein-, amino sugar-, cellulose-, lignin-, and black carbon-like character, along with potential structural information such as aliphatic and phenolic moieties.[13–15] NOM from marine, freshwater, and glacial ecosystems is comprised of chemical constituents that are polyfunctional, heterogeneous, polyelectrolytic, vary in molecular weights, and is present at high and low concentrations. High magnetic field

* *Correspondence to*: J. D'Andrilli, Department of Chemical and Biological Engineering, 366 EPS Building, Montana State University, Bozeman, MT 59717, USA.
E-mail: Juliana@montana.edu

(>7 tesla) ultrahigh-resolution Fourier Transform Ion Cyclotron Resonance Mass Spectrometry (FTICRMS)[16] is currently the only mass spectrometry technique capable of achieving the resolution and accuracy required to directly determine molecular formulae of NOM constituents. High field strength and field homogeneity are the keys to produce both ultrahigh mass resolving power ($m/\Delta m_{50\%}$ >500,000, in which $\Delta m_{50\%}$ is the mass spectral peak full width at half-maximum peak height) and mass accuracy (rms error <1.0 ppm) for compositionally complex NOM. Within the last two decades, great strides have been made with FTICRMS in chemically characterizing NOM samples from environments worldwide that were never before probed at the molecular level. FTICRMS advances mainly affect which molecular species are observed, not the mass accuracy on which the elemental composition assignments are based. Confirming specific naturally occurring isotopic mass spacing patterns for complex NOM elemental compositions, such as $C_cH_hN_nO_oS_s$, thus extended our analytical understanding of NOM beyond just $C_cH_hO_o$ components.

Because NOM constituents represent various chemical classes, it has been, and continues to be, effective to visualize and interpret FTICRMS molecular data with van Krevelen diagrams, namely, plots of atomic H/C versus O/C ratios.[9] NOM typically exhibits hydrogen saturation and oxygenation as $0 < H/C < 2.5$ and $0 < O/C < 1.2$. In a van Krevelen plot, NOM species typically cluster into regions corresponding to compound classes and aromatic nature in various references.[9,10,13,17–19] Extending those observations further, Kim *et al.*[9] also proposed identification of possible chemical reaction pathways visualized from a van Krevelen diagram, for particular ranges of H/C and O/C ratios. That information can then be used to determine OM sources, evolution, microbial influence, degree of hydrogen, carbon, and oxygen saturation, and potential structural families to assess the role of organic carbon in an environment. Taken together, a great deal of information of NOM characterization by FTICRMS has been gained by graphical interpretation of van Krevelen diagrams and continues to evolve today.[15]

Recent ultrahigh-resolution FTICRMS studies of microbially derived NOM reinforce the value of van Krevelen diagrams as a reflection of the chemical character of the NOM that is similar to the labeled class regions.[18] For example, microbially derived, bioavailable fractions, therefore classified as more labile NOM, have been linked to high H/C and low O/C ratios in the lipid-, protein-, and amino sugar-like regions of the van Krevelen digram.[18,20–23] NOM constituents grouped in such regions also contain a high percentage of heteroatoms: $C_cH_hN_nO_oS_s$ species that function as electron donors for microbial metabolism and/or are metabolic intermediates and products.

It should be noted that OM from Pony Lake, Antarctica, contains no higher plant (lignin), allochthonous inputs and is therefore completely microbially derived. Nevertheless, OM produced in microbial metabolism at Pony Lake exhibits compositional classes similar to those from terrestrially derived lignin-like material, as seen from the van Krevelen diagram, and thus shares the chemical reactivity in that region in common with Suwannee River fulvic acid.[18] The difference between autochthonous, microbially derived OM and allochthonous freshwater, terrestrially derived and more recalcitrant OM, was addressed in that work, touching on the concept of more versus less labile OM nature from each source. The question then remains; can we use FTICRMS-derived elemental compositions to determine the extent of labile versus recalcitrant nature of NOM in marine, freshwater, and glacial environments?

Determining the fate of more and less labile OM in the environment remains a chemical and biological controversy; however, in this study, we address this continuing dialogue and aim to identify chemical molecular information to define NOM labile nature that can be used to provide insight into physical, chemical, and biological processing in the environment. Battin *et al.*[12] define labile NOM constituents as bioavailable carbon that is utilized in heterotrophic activity. Therefore, environmental processing of labile NOM contributes to the global carbon cycle; production and release of OM can increase CO_2 concentration in the atmosphere.[12] Direct measurements on the labile nature of NOM in marine, freshwater, and glacial environments is achieved by studying *in situ* microbial processing of NOM constituents over time, which can be labor intensive and costly. As multiple complementary techniques are commonly employed to extensively characterize various NOM fractions in different ecosystems with or without *in situ* experimentation, the present objective is to focus solely on a new interpretation of molecular data generated by ultrahigh-resolution FTICRMS to extend our current understanding of the labile nature of NOM in various environments, when other biological information is not available. A single ultrahigh-resolution FTICR mass spectrum of NOM could serve as a surrogate for time-consuming bioavailability studies; biological assays on NOM bioavailability based on respiration or other processing by bacteria can extend to multiple weeks and months.[6]

Here, we introduce a specific molecular lability index by use of many ultrahigh-resolution FTICRMS datasets, both new and previously published, to incorporate this novel analysis based on the chemical composition of NOM samples to distinguish between more and less labile molecular constituents. The degree of lability would therefore link to more or less bioavailable species of OM detectable by FTICRMS, the microbial biological processing of carbon within ecosystems, and could also be used to compare across ecosystems. The proposed molecular lability boundary (MLB) divides the data into two groups encompassing more or less labile material, derived from calculated hydrogen saturation molecular values that group together within three different chemical regions (lipid-, protein-, and amino sugar-like) in van Krevelen diagrams, previously classified with stronger microbial influence and linked to more labile nature.[23–25] We have selected molecular data determined by FTICRMS over the last decade from multiple environments to validate the MLB, including OM studies investigating microbial abundance, microbial community, and respiration rates of specific microbes. We considered marine, freshwater, and glacial environments for this work, to span a range of ecosystems investigated by FTICRMS.

Rapid Communications in Mass Spectrometry

EXPERIMENTAL

Samples and sample preparation

To develop and authenticate the MLB, a diverse set of environmental OM samples was chosen from marine, estuarine, freshwater, and glacial ecosystem OM data generated from the same mass spectrometer instrument between 2005 and 2015 (Table 1). Marine environments included the New Zealand Subtropical Convergence, Antarctic Weddell Sea bottom water and sea-ice brine, and the Gulf of Mexico (USA). Estuarine samples were obtained from Cape Fear, North Carolina, and from the Apalachicola River, Florida, at the junction where the river meets the coastal bay before mixing with the Gulf of Mexico (USA). The freshwater environment samples span parts of the USA and New Zealand, including Suwannee River fulvic acid (International Humic Substance Society; IHSS), northern Minnesota peatland porewaters of the Glacial Lake Agassiz Peatlands (GLAP), the Black River, North Carolina, and the Freshwater River and Doubtful Sound of New Zealand. Finally, both glacial ecosystem OM samples were collected from Antarctica: Pony Lake (fulvic acid, IHSS) and the Cotton Glacier (CG) supraglacial stream. OM was isolated from each environment and prepared for FTICRMS by solid-phase extraction (SPE; PPL Varian Mega Bond Elut and Agilent Technologies), which concentrates OM efficiently and removes inorganic salt matrices. Although sample preparation methods, such as SPE and freeze drying, can have a molecular bias and a somewhat selective view of the total dissolved OM pool, these methods are commonly applied in organic geosciences to observe molecular

Table 1. Sample information of all organic matter samples analyzed between 2005 and 2015 by 9.4 tesla ESI-FTICRMS at the National High Magnetic Field Laboratory, in Tallahassee, Florida

Environment	Sample Name	Location	OC Concentration	Reference	Notes
Marine	Subtropical Convergence	South Island, New Zealand	50–70 μM	38	Sampling stations STC01, STC04, and STC08 in austral summer and winter
	Weddell Sea Bottom Water	Antarctica		34,52	Collected from the ANT XXII/2 expedition of the RV/V Polarstern
	Gulf of Mexico	USA	49 μM	This study, 23,26	Bush Hill cold hydrocarbon seep, deep ocean brine, and bottom water
	Gulf of Mexico Algal DOM	USA	500 μM	This study and 23	Isolated marine algal OM before and after passage through sand columns
Marine / Glacial	Weddell Sea sea-ice Brine	Antarctica		34,52	Collected from the ANT XXII/2 expedition of the RV/V Polarstern
Estuarine	Cape Fear	North Carolina, USA	630–651 μM	25	Samples collected and split into before and after 21 h irradiation
	Apalachicola River	Gulf of Mexico, USA	615 μM	This study and 67	Riverine mature OM sample that meets the Apalachicola Bay
Terrestrial Freshwater	Suwannee River	Georgia, USA	42 mM	This study and 18	IHSS Fulvic Acid and RO NOM
	Red Lake II Peatland Porewater	Minnesota, USA	3.10–7.10 mM	This study and 37	Fen and bog porewaters collected at the surface and at depth
	Lost River Peatland Porewater	Minnesota, USA		This study	Bog porewaters collected at the surface and at depth
	Black River	North Carolina, USA	930–965 μM	25	One sample collected and split into before and after 21 h irradiation
	Freshwater River	Stewart Island, New Zealand	200–400 μM	This study and 55	Samples collected with varying salinity gradients
	Doubtful Sound	South Island, New Zealand		This study and 55	Samples collected with varying salinity gradients
Glacial	Pony Lake	Antarctica	42 mM	18	IHSS Fulvic Acid
	Cotton Glacier Supraglacial Stream	Antarctica	0.017 μM*	This study	Collected in austral summer and concentrated by reverse osmosis

*Note: OC concentration was measured by a total organic carbon analyzer from Shimadzu Scientific (TOC-V series).

characterizations of OM by FTICRMS and to estimate ecosystem relevance. SPE continues to be the most widely used OM extraction technique with PPL cartridges reported as the most effective sorbent for OM extraction over a vast range of environments.[19] PPL SPE cartridges were thus selected based on their documented ability to extract a wide range of polar and nonpolar OM constituents from the environment and for their high extraction efficiencies compared to other SPE sorbents for NOM.[26]

OM extracts were eluted with HPLC grade methanol and stored in the dark in clean, combusted amber glassware at or below 4 °C prior to analysis. Sample volume varied depending on availability, OM concentration, and PPL SPE cartridge carbon loading instructions (details provided in Dittmar *et al.*[26]). All samples listed in Table 1 were prepared by SPE except for the Minnesota peatland samples collected at Lost River bog that were freeze-dried and reconstituted in methanol prior to FTICRMS analysis.

Electrospray ionization (ESI)

Detection of charged gaseous ions by FTICRMS requires an external ionization method. Singly charged, negative gaseous ions were produced by a custom-built micro-electrospray ionization source.[27] A range of experimental parameters is reported for all OM samples: 50 µm i.d. fused-silica tube, syringe pump flow rate 0.5–1.0 µL/min, needle voltage –2500 V or –2700 V, tube lens –325 to –350 V, and heated metal capillary operated at 7.21–11.5 W. Positive ESI and atmospheric pressure photoionization were also considered for these comparisons, but, for the purpose of this study, were not included due to the more extensive use of negative ESI-FTICRMS analysis of a broad range of environmental NOM samples.

9.4 tesla FTICRMS

Data considered for this work were obtained between 2005 and 2015, with a custom-built 9.4 tesla superconducting magnet FTICR mass spectrometer at the National High Magnetic Field Laboratory (NHMFL) in Tallahassee, Florida, USA.[28,29] Excitation ranged from *m/z* 200–1500 at frequency sweep 50 Hz/µs, and octopole ion guide frequencies were maintained between 1.5–2.0 MHz. Both ESI and FTICRMS parameter ranges incorporate ten years of 9.4 tesla FTICRMS acquisition at the NHMFL, and were selected based on previously characterized NOM samples and optimized for each study. For mass spectral generation, multiple (50–200) time domain acquisitions were co-added, Hanning apodized, and zero-filled once before fast Fourier transformation and magnitude calculation.[30]

Mass spectral calibration and molecular formula assignment

Both external and internal calibrants were utilized for FTICRMS NOM characterization over the last ten years. In the earlier years, external calibrant solutions and NOM samples were ionized and separately introduced into the mass spectrometer by dual spray ESI. Mass spectra were then generated of combined coadditions of NOM and calibrant solution experiments. Spectra were calibrated from the known molecular formulae for the calibrant peaks and applied for all mass-to-charge ratios. Currently, mass spectra are calibrated internally with at least two homologous -CH_2 series commonly found in NOM, spanning $200 < m/z < 700$; therefore, an external calibrant solution is not typically necessary. Homologous series commonly used for NOM calibration were detected for NOM from vastly different environments by FTICRMS, ranging from marine to freshwater ecosystems, including glaciated environments. Both types of calibration yield assigned elemental compositions with rms mass measurement error <1 ppm for singly charged negative OM analyte ion species when assigning molecular formulae. Peak lists were generated by NHMFL software for molecular formula assignment, limited to peaks of magnitude greater than 6× the baseline rms noise – a conservative threshold that allows for reliable comparison of NOM from different sources. OM samples for this study were determined to be singly charged by confirming the naturally occurring ^{13}C-isotopic FTICRMS peak separation (*m/z* 1.0034) between ions differing in elemental composition by $^{12}C_c$ vs. $^{12}C_{c-1}$-$^{13}C_1$.[31–33]

NOM molecular formula assignment by 9.4 tesla ESI-FTICRMS analysis has been previously described in detail.[18,20,34] Compositional constraints were modeled after those reported for NOM characterization by FTICRMS and elemental compositions containing either $C_cH_hO_o$ or $C_cH_hN_nO_oS_s$ were considered for this work.[18,20,34] Also, hydrocarbon molecular assignments without incorporating O assignment in the NOM molecular backbone were not considered for this comparative study.

The correct identification of OM molecular constituents containing $C_cH_hN_nO_oS_s$ is impossible without various confirmation steps based on mass defects, naturally occurring isotopic mass spacing patterns (previous example: ^{12}C and ^{13}C), homologous series, and rms error less than 1 ppm. Every compound of elemental composition $C_cH_hN_nO_oS_s$ exhibits a unique mass defect, defined as the difference between the exact molecular mass and the nearest integer ("nominal") mass. Therefore, each $C_cH_hN_nO_oS_s$ OM species can be unambiguously assigned a correct molecular formula from its experimentally determined *m/z* value (singly charged molecular species have $z = 1$). Confirmation of correctly identified $C_cH_hN_nO_oS_s$ species within a possible empirical molecular formula is achieved by identifying species of the same chemical formula, but with a heavy atom isotope (^{2}H, ^{13}C, ^{15}N, ^{18}O, ^{34}S) in place of the most abundant isotope (^{1}H, ^{12}C, ^{14}N, ^{16}O, ^{32}S). Although species containing phosphorus have been reported in specific types of OM samples by nuclear magnetic resonance spectroscopy,[35,36] phosphorus occurs naturally only as ^{31}P, so its identification in a chemical formula must rely solely on assignment of other molecular monoisotopic species.

Inspecting isotopic mass spacing patterns and setting molecular formula assignment restrictions are necessary to exclude incorrect molecular formula assignments by FTICRMS; specific restrictions for NOM containing $C_cH_hN_nO_oS_s$ have been previously outlined.[18,34] For all OM samples, negatively charged ion masses were converted into neutral masses for molecular formula assignment and comparison, as in the past for NOM characterization by FTICRMS at NHMFL.[23,25,37,38] Also, we defined the molecular backbone of NOM to contain only $C_cH_hO_o$ and classified elemental combinations of N and S to further define its heterogeneity.

Rapid Communications in Mass Spectrometry

RESULTS AND DISCUSSION

Molecular lability boundary: definition and examples

Ultrahigh-resolution FTICRMS is the only advanced analytical technique that is capable of resolving most of the separable OM molecular components. Thus, this technique remains unrivaled in its ability to produce an ultrahigh-resolution molecular dataset encompassing a sizable analytical window of the OM pool in the environment. Large OM FTICRMS molecular datasets (>5000 MS peaks) are effectively visualized from van Krevelen diagrams. The concept of an FTICRMS molecular lability boundary (MLB) is based on our current understanding of van Krevelen diagrams, incorporating chemical information depicted by various H/C and O/C ratios and the relative boundaries of each chemical class region (Figs. 1(a)–1(f)).[9,15,17–19] Chemical class regions from van Krevelen diagrams are used to depict NOM qualitative characterizations of molecular data that comprise ultrahigh-resolution FTICR mass spectra,[9] and the same general classes were used to consistently compare the NOM quality across all samples. Regions of protein-, amino sugar-, and lipid-like OM character at higher degrees of hydrogen saturation have been linked to more bioavailable fractions of carbon.[18,20–23] The MLB extends the relevance of ultrahigh-resolution FTICRMS analysis beyond chemical formula determination, thereby expanding the interpretation of van Krevelen diagrams toward further prediction of biogeochemical properties.

Even before van Krevelen diagrams became widely used to efficiently project the thousands of formulae identified by FTICRMS onto an easily understood 2-D plot, it had been

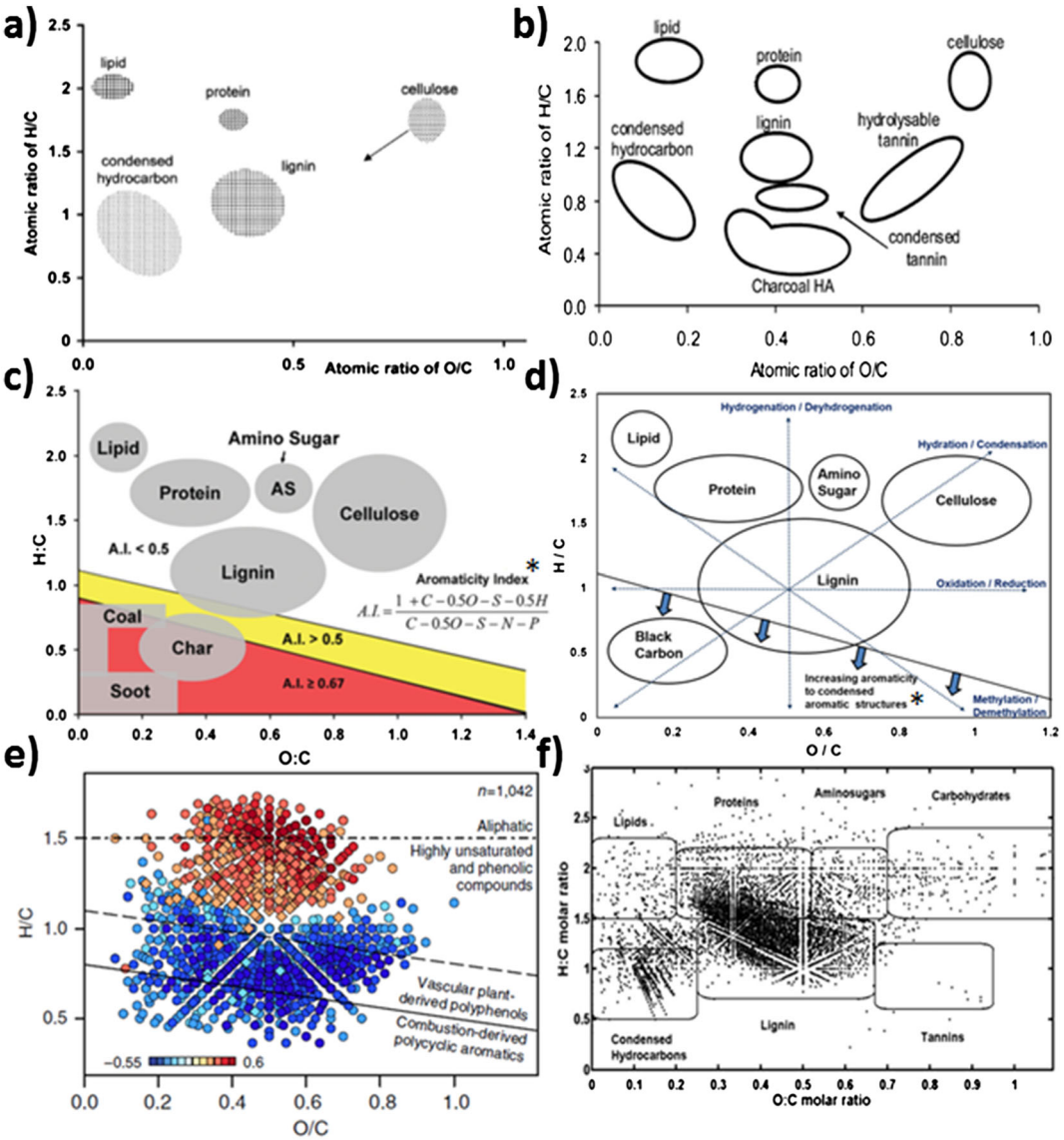

Figure 1. Examples of van Krevelen diagrams depicting chemical class regions and their relative boundaries generated over a 11-year period from (a) Kim *et al.*;[9] (b) Mopper *et al.*;[10] (c) Podgorski *et al.*;[17] (d) D'Andrilli *et al.*;[18] (e) Swedish boreal lake OM where diamond symbols correspond to molecular formulae containing N in Kellerman *et al.*;[15] and (f) Lake Superior surface water OM in Minor *et al.*[19] *Aromaticity index derived from Koch and Dittmar.[13]

recognized that labile and recalcitrant NOM differed in their elemental H/C and O/C ratios. Perdue and Ritchie,[39] for example, summarized bulk O/C and H/C ratios of humic acids, fulvic acids, and NOM reported by Shapiro[40] and determined by traditional combustion techniques. They pointed out that these largely recalcitrant compounds exhibited lower H/C and to some extent higher O/C ratios than their biomass precursors. Perdue and Ritchie explained these observations in the context of carbon oxidation state, noting that the major fractions of precursor biomass (lipids, proteins, sugars, and lignin) exhibited average carbon oxidation states of less than 1, whereas carbon oxidation states in humic substances and NOM ranged from +0.25 to +0.33.

Additional evidence for a link between elemental ratios and OM lability was presented by Osborne *et al.*[41] in their study of dissolved organic nitrogen (DON) bioavailability. Five-day bioassays of riverine water enriched in DON from agricultural sources indicated that the reactive organic nitrogen compounds had formulas generally higher in H/C and lower in O/C than the compounds that were produced, indicating that more saturated, less oxygenated molecules were bioavailable. These data also suggested that the microbes were converting lipid- and protein-like N-containing compounds into more oxygenated and less hydrogenated (more unsaturated) structures that still contain N and that were largely recalcitrant. That is, microbes changed the carbon skeleton of the reactive DON fraction, but without concomitant consumption of N.

The MLB, therefore, is also based on the calculated hydrogen saturation (H/C) values of OM molecular formulae. With this dividing threshold, the number of OM constituents are separated by the MLB at H/C ≥1.5, corresponding to more labile molecular formulae in more bioavailable chemical class regions (shaded regions on all subsequent figures), and H/C <1.5, representing less labile, more recalcitrant chemical nature (grouping in more lignin-, tannin-, and condensed aromatic-like regions of the van Krevelen diagram) over all O/C ratios. The MLB at H/C = 1.5 is drawn at the bottom of the chemical class boundaries linked to NOM bioavailability, which is the boundary condition between aliphatic chemical species and the group of highly unsaturated and phenolic compounds from a van Krevelen diagram.[15] Examples of previously published reference van Krevelen diagrams with chemical class descriptions are presented in Figs. 1(a)–1(f), spanning more than a decade of FTICRMS OM chemical characterization information generated and expanded upon over time. Figures 1(e) and 1(f) show FTICRMS molecular data from Swedish boreal lakes containing molecular formulae with (◊) and without (○) N atoms, with dashed lines dividing the chemical data into structural groups, and extracted OM from a Lake Superior surface water, respectively. Within the last decade, OM characterization has extended beyond the molecular backbone of $C_cH_hO_o$ to include heteroatomic molecular species. Here, we report NOM molecular data containing combinations of $C_cH_hO_o$ and $C_cH_hN_nO_oS_s$, each element confirmed with monoisotopic mass spectral patterns, to develop the MLB. The MLB extends our current interpretation of FTICRMS molecular data, providing a rapid ultrahigh-resolution advanced metric to assess NOM molecular information and bioavailability simultaneously. Percentages of labile and recalcitrant components can also be calculated for each heteroatom group (different molecular species containing $C_cH_hN_nO_oS_s$ when n = 0, 1, 2 and s = 0 or 1).

The percentage of more labile constituents is determined by the number of molecular formulae having H/C ≥1.5 over all O/C (0.0–1.2) divided by the total amount of molecular formulae in the sample or by the number of formulae in a heteroatom group (containing molecular constituents beyond C, H, and O defining heterogeneous lability), multiplied by 100. Classification of less labile, more recalcitrant components from each carbon source is calculated similarly for molecular formulae below the MLB, corresponding to molecular species that cluster in more lignin-, tannin-, and black carbon-like regions of the van Krevelen diagram (H/C <1.5). These calculations are defined as chemical species richness for more labile or more recalcitrant contributions (MLB_L and MLB_R). As stated previously, the chemical class regions in van Krevelen diagrams contain a degree of ambiguity and therefore do not define exact borders of molecular data.[18] Even so, this conservative MLB calculation can be used as a relatively unbiased method to distinguish between more or less labile NOM by FTICRMS. Expanding beyond richness, diversity of chemical species was calculated by incorporating the normalized peak height of each mass spectral peak to determine the weighted effect of each ionized elemental composition to the overall distribution in each group (i.e., labile: MLB_{wL} or recalcitrant: MLB_{wR}).

Although we define a zero slope hydrogen saturation MLB (encompassing the more bioavailable character of carbon in lipid-, protein-, and amino sugar-like regions), we acknowledge that the degree of lability can also be a function of oxygenation. Therefore, gradients can exist within the two grouped regions of labile and recalcitrant OM nature. Above the MLB, we submit that molecular lability increases with decreasing oxygenation and increasing hydrogenation (highest H/C and lowest O/C ratios) and also decreases with increasing oxygenation for which molecular constituents are found to group in the cellulose-like region of the diagram. Moreover, the most recalcitrant OM exhibit the lowest H/C ratios and the lowest O/C ratios, in the region commonly referred to as black carbon-like (i.e., the most condensed aromatic lignin-like OM). Known to represent OM constituents that accumulate in the environment over time, these species are the most challenging OM to process in the environment.[42]

For each OM sample, FTICRMS molecular data was used to calculate richness and diversity contributions above and below the MLB to determine the extent of labile components across all ecosystems (Table 2). Labile percentages ranged from zero to 46.5, with OM from the supraglacial CG stream (Antarctica) as the most labile and OM from Cape Fear (North Carolina) before and after irradiation and Freshwater River of Stewart Island (New Zealand) as the most recalcitrant. All environments contained a higher ratio of recalcitrant richness. Glacial environments generally contain more labile OM, followed by marine and freshwater ecosystems. Glacial environments are hypothesized to be the most labile among the listed classifications in Table 1, due to the predominant microbial influence on the OM located in protein- and amino sugar-like regions at higher H/C ratios. Note that molecular formulae below the MLB can include OM from both autochthonous and allochthonous

Rapid Communications in Mass Spectrometry

Table 2. Organic matter samples from various environments ranked from most labile to least labile by applying the molecular lability boundary to calculate richness (MLB_L and MLB_R) and mass spectral peak height weighted distribution percentages (MLB_{wL} and MLB_{wR}) for labile and recalcitrant contributions

	Richness		Diversity Distribution	
Sample Name	**% MLB_L**	**% MLB_R**	**% MLB_{wL}**	**% MLB_{wR}**
Cotton Glacier Stream	46.5	53.5	68.6	31.4
Algal Marine-Derived OM before sand filtration	38.8	61.2	27.2	72.8
Weddell Sea sea-ice Brine	28.4	71.6	18.2	81.8
Algal Marine-Derived OM mixture after sand filtration	21.8	78.2	34.4	65.6
Pony Lake Fulvic Acid	20.8	79.2	17.4	82.6
Subtropical Convergence: near coast (summer)	17.8	82.2	9.79	90.2
Subtropical Convergence: center (summer)	14.6	85.4	7.65	92.3
Subtropical Convergence: near coast (winter)	14.1	85.9	8.12	91.9
Gulf of Mexico: Brine Pool	13.8	86.2	10.4	89.6
Subtropical Convergence: SubAntarctic Surface Water (summer)	12.9	87.1	7.04	92.9
Doubtful Sound (salinity 34.21)	12.2	87.8	5.02	94.9
Subtropical Convergence: center (winter)	10.1	89.9	6.09	93.9
Subtropical Convergence: SubAntarctic Surface Water (winter)	10.1	89.9	6.00	94.0
Doubtful Sound (salinity 10.30)	9.51	90.5	4.20	95.8
Weddell Sea Bottom Water	8.98	91.0	3.71	96.3
Minnesota Lost River Deep Bog	7.93	92.0	4.69	95.3
Gulf of Mexico: Bottom Water	7.89	92.1	3.18	96.8
Suwannee River Fulvic Acid	7.67	92.3	4.06	95.9
Gulf of Mexico: Bush Hill (hydrocarbon cold seep)	7.14	92.9	2.46	97.5
Suwannee River NOM	6.72	93.3	2.82	97.2
Black River Irradiated	5.02	94.9	2.36	97.6
Freshwater River, Stewart Island (salinity 5.00)	4.90	95.1	1.37	98.6
Minnesota Lost River Surface Bog	4.60	95.4	2.17	97.8
Freshwater River, Stewart Island (salinity 28.00)	4.35	95.6	1.43	98.6
Minnesota Red Lake II Deep Fen	3.33	96.6	1.58	98.4
Minnesota Red Lake II Deep Bog	3.22	96.8	1.13	98.9
Minnesota Red Lake II Surface Fen	2.57	97.4	1.87	98.1
Apalachicola River outlet to bay of Gulf of Mexico	2.31	97.7	0.683	99.3
Minnesota Red Lake II Surface Bog	2.06	97.9	0.699	99.3
Freshwater River, Stewart Island (salinity 14.00)	2.00	98.0	1.94	98.1
Black River before Irradiation	1.94	98.1	0.563	99.4
Doubtful Sound (salinity 0.00)	0.393	99.6	0.158	99.8
Cape Fear Irradiated	0	100	0	100
Cape Fear before Irradiation	0	100	0	100
Freshwater River, Stewart Island (salinity 0.00)	0	100	0	100

sources, and thus should not be exclusively linked to higher plant or lignin inputs. Pony Lake fulvic acid provides a good example of microbially derived OM with higher and lower degrees of hydrogen saturation.[18]

The MLB_{wL} calculation also produced the same overall trend observed for richness in which CG stream OM was ranked as the most labile environment (68.6%) and both Cape Fear OM samples and the Freshwater River (0.00 salinity) were ranked as the most recalcitrant (0%; Table 2). Here the distributions of MLB_w provide a measure of how the differences in elemental composition peak abundance, within the labile and recalcitrant groups, further define its character in the environment.

Even though CG OM was ranked as the most labile sample, it is still considered to have more overall recalcitrant nature (53.5%). However, applying the MLB_w to the FTICRMS data reveals the opposite relationship for CG OM: a greater percentage of labile (68.6%) to recalcitrant (31.4%) constituents and was the only environment dominated by labile OM species considering all 35 samples. Thus, the contribution of MLB_{wL} molecular species within the MLB_L to the overall CG OM chemical character was greater than within the MLB_R, with the most abundant species contribution from $CHOS_1$. To easily visualize how the OM directly compares in labile nature, chemical character, molecular heterogeneity, and diversity contribution, composition and lability data for each molecular group was tabulated (Tables 3–7) and van Krevelen diagrams were generated (Figs. 2–6) for each unique environment sampled as a part of this study. Clear differences in labile nature are observed for OM from various environments, with varying heterogeneous nature, environmental features, and gradients of algal processing, salinity, irradiation, seasonality, and depth. Heterogeneous character is defined here by the heteroatomic content, that is, the number of formulae that contain N and S in addition to C, H, and O. Data in Tables 3–7 suggest that these heteroatomic N- and S-containing molecular species contribute considerably to the labile character of OM from each environment.

Table 3. Gulf of Mexico organic matter (OM) molecular species and labile nature contributions before (algal marine-derived OM and mature riverine OM) and after (mixture of algal and riverine OM) natural sand filtration in coastal sediments

	Algal Marine-Derived OM			Mixture of Algal and Riverine OM			Mature Apalachicola Riverine OM		
Molecular species	Composition (%)	MLB_L (%)	MLB_R (%)	Composition (%)	MLB_L (%)	MLB_R (%)	Composition (%)	MLB_L (%)	MLB_R (%)
CHO	33.4	55.1	44.9	63.2	26.1	73.9	70.9	2.03	98.0
$CHOS_1$	27.7	40.9	59.1	12.0	33.3	66.7	16.2	5.41	94.6
$CHON_1$	11.4	46.5	53.5	15.4	5.44	94.6	10.7	0	100
$CHON_1S_1$	16.1	12.5	87.5	0	0	0	0	0	0
$CHON_2$	2.80	8.91	91.1	9.37	4.72	95.3	2.15	0	100
$CHON_2S_1$	8.56	17.2	82.8	0	0	0	0	0	0
Overall		**38.8**	**61.2**		**21.8**	**78.2**		**2.31**	**97.7**

Table 4. Gulf of Mexico bottom water feature (brine fluid seep, a hydrocarbon and oil seep [Bush Hill], and bottom water sample without any seep influence), and Antarctic Weddell Sea feature (sea-ice brine and bottom water) organic matter percent composition and lability

	Brine Pool			Bottom Water			Bush Hill		
Molecular Species	Composition (%)	MLB_L (%)	MLB_R (%)	Composition (%)	MLB_L (%)	MLB_R (%)	Composition (%)	MLB_L (%)	MLB_R (%)
CHO	36.8	14.0	86.0	49.3	9.35	90.6	50.5	9.31	90.7
$CHOS_1$	22.3	31.6	68.4	15.3	20.0	80.0	13.7	17.1	82.9
$CHON_1$	23.8	4.88	95.1	19.5	0.587	99.4	20.5	0.209	99.8
$CHON_1S_1$	7.85	5.06	94.0	2.90	3.95	96.1	1.92	0	100
$CHON_2$	9.29	0	100	12.3	0	100	13.4	0.319	99.7
$CHON_2S_1$	0	0	0	0.762	0	100	0	0	0
Overall		**13.8**	**86.2**		**7.89**	**92.1**		**7.14**	**92.9**
	Weddell Sea Sea-ice Brine			**Weddell Sea Bottom Water**					
Molecular Species	Composition (%)	MLB_L (%)	MLB_R (%)	Composition (%)	MLB_L (%)	MLB_R (%)			
CHO	42.7	22.9	77.0	45.3	9.46	90.5			
$CHOS_1$	27.0	54.6	45.4	18.1	23.3	76.7			
$CHON_1$	15.1	8.92	91.1	18.8	0.630	99.4			
$CHON_1S_1$	6.16	40.1	60.2	4.91	6.37	93.6			
$CHON_2$	8.43	0	100	11.2	0	100			
$CHON_2S_1$	0.595	0	100	1.22	0	100			
$CHON_3$	0	0	0	0.337	0	100			
Overall		**28.4**	**71.6**		**8.94**	**91.0**			

Natural OM processing in the Gulf of Mexico coastal sands

FTICRMS molecular formulae were determined for OM in a series of degradation experiments through coastal permeable shelf sediments to reveal the fate of Apalachicola River OM as it enters the Apalachicola Bay before reaching the Gulf of Mexico.[23] Three samples from that study were analyzed here: Apalachicola River OM (collected at the outlet of the Apalachicola River where it meets the Apalachicola Bay), an algal marine-derived OM sample (diatom lysate: *Thalassiosira* sp.), and a mixture of Apalachicola River and algal marine-derived OM after heterotrophic processing in a laboratory-engineered sand column.[23] The algal marine-derived OM and the mixture samples both contained a higher percentage of more labile constituents reflecting more hydrogen-saturated species relative to other OM environments (Table 2), predicted for microbially derived OM (38.8% and 21.8% MLB_L). However, the MLB_{wL} values were reversed, with the greatest contribution of molecular species in the labile region for the OM mixture after column exposure (CHO molecular species as the greatest contributor within the group).

The percent composition of molecular species and percent MLB_L for the algal marine-derived OM and mixture samples (after column exposure) were very different, capturing the heterogeneous molecular species shifts in this coastal sand OM mineralization experiment (Table 3). Apalachicola River OM was the least heterogeneous and the most recalcitrant of these three samples (70.9% CHO and 97.7% MLB_R), comprised of mostly lignin- and tannin-like material,[23] as expected for a mature freshwater OM environment.

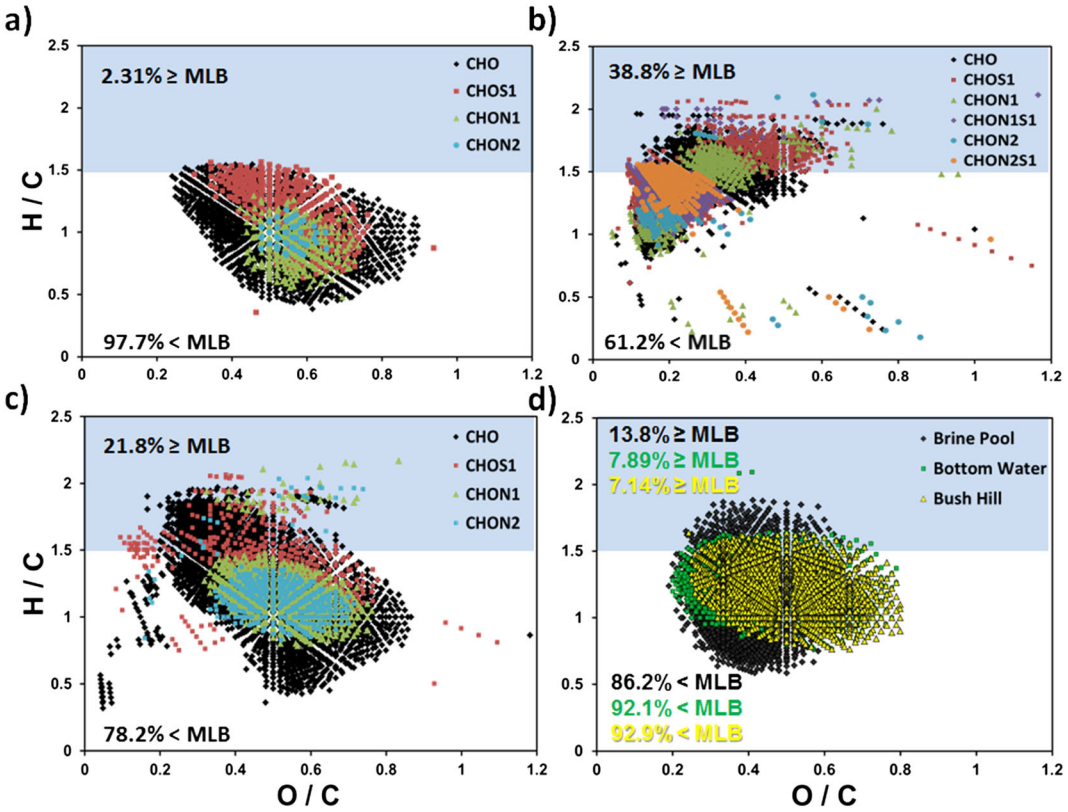

Figure 2. van Krevelen diagrams for organic matter (OM) isolated from (a) the Apalachicola River; (b) marine algae before passage through a laboratory engineered sand column; (c) the mixture of algal marine-derived and Apalachicola River OM after passage through the sand column; and (d) Gulf of Mexico brine fluid seep, hydrocarbon and oil seep (Bush Hill), and bottom water.

Heterogeneous molecular species above and below the MLB are shown in van Krevelen diagrams (Figs. 2(a)–2(c)). Overall, hydrogen saturation decreased and oxygenation increased after microbial processing of the OM in the column. The most noticeable shifts in oxygenation occurred for every heteroatom-containing molecular species, with the exception of $CHON_1S_1$ and $CHON_2S_1$, which did not appear after column exposure. After sand filtration in the column, the OM character in Fig. 2(c) shows distinct similarities to the Apalachicola River OM (Fig. 2(a)), yet still exhibits more species above the MLB at higher hydrogen saturation and thus is more labile comparatively. The higher MLB_{wL} values for the OM mixture after column exposure may be attributed to a greater percentage of CHO-containing species (28.9%) produced from the natural microbial processing occurring within the column compared to the same molecular species of algal marine-derived OM before column exposure (13.3%). These CHO components detected after column exposure clearly fall within the lipid-, protein-, and amino sugar-like regions of the van Krevelen diagram.

Gulf of Mexico benthic OM characterization

The Gulf of Mexico is a unique ecosystem, with bottom waters influenced by oil, gas, and brine fluid seeps.[43–45] Three separate Gulf of Mexico sample sites were selected to capture different bottom water environments for various biological and chemical studies: brine pool (brine fluid seep), Bush Hill (oil and methane seep), and a bottom water control sample.[26,46] Brine pool OM contained the most heterogeneous molecular composition and also the most labile nature (Table 4). The Gulf of Mexico brine pool is characterized by a pocket of symbiotic bacteria and mussels;[47] therefore, a higher degree of labile nature due to microbial metabolism was expected. Note that Bush Hill OM had the least labile nature, containing the least hydrogen saturation and most carbon unsaturated species of all of the Gulf of Mexico samples (MLB_L: 7.14%), which was unexpected in view of the existing hydrocarbon seep and bacterial contributions.[46,48,49] Sulfide-oxidizing bacteria at Bush Hill produce sulfoxide OM[46] resulting in a localized environment containing the highest contribution of heteroatomic species (MLB_L of $CHOS_1$: 17.1%) to its overall OM labile nature.

Similarities and differences in the Gulf of Mexico OM chemical character of each sample are illustrated in Fig. 2(d). Bush Hill and bottom water shared very similar OM character centered at H/C: 1.0–1.25 and O/C: 0.5, in the lignin-like region of the van Krevelen diagram. Both samples varied more in the degree of oxygenation than hydrogen saturation. Brine pool OM extended to higher H/C ratios for MLB_L, having the most labile character, but also has molecular species at the lowest H/C ratios, characteristic of more condensed aromatic nature. Varying the most in chemical character, the brine pool environment produced many different types of OM, which we attribute to the diverse group of symbiotic organisms that depend on and benefit from the brine fluid seep.[47]

Table 5. North Carolina freshwater and estuarine percent composition and lability for organic matter before and after irradiation exposure

	Black River before irradiation			Black River after irradiation		
Molecular species	Composition (%)	MLB_L (%)	MLB_R (%)	Composition (%)	MLB_L (%)	MLB_R (%)
CHO	63.6	1.48	98.5	70.1	5.58	94.4
$CHOS_1$	16	6.22	93.8	11.8	9.09	90.9
$CHON_1$	16	0	100	18.1	0.181	99.8
$CHON_1S_1$	0.057	0	100	0	0	0
$CHON_2$	4.3	0	100	0	0	0
Overall		**1.94**	**98.1**		**5.02**	**94.9**
	Cape Fear before irradiation			**Cape Fear after irradiation**		
Molecular species	Composition (%)	MLB_L (%)	MLB_R (%)	Composition (%)	MLB_L (%)	MLB_R (%)
CHO	100	0	100	100	0	100
Overall		**0**	**100**		**0**	**100**

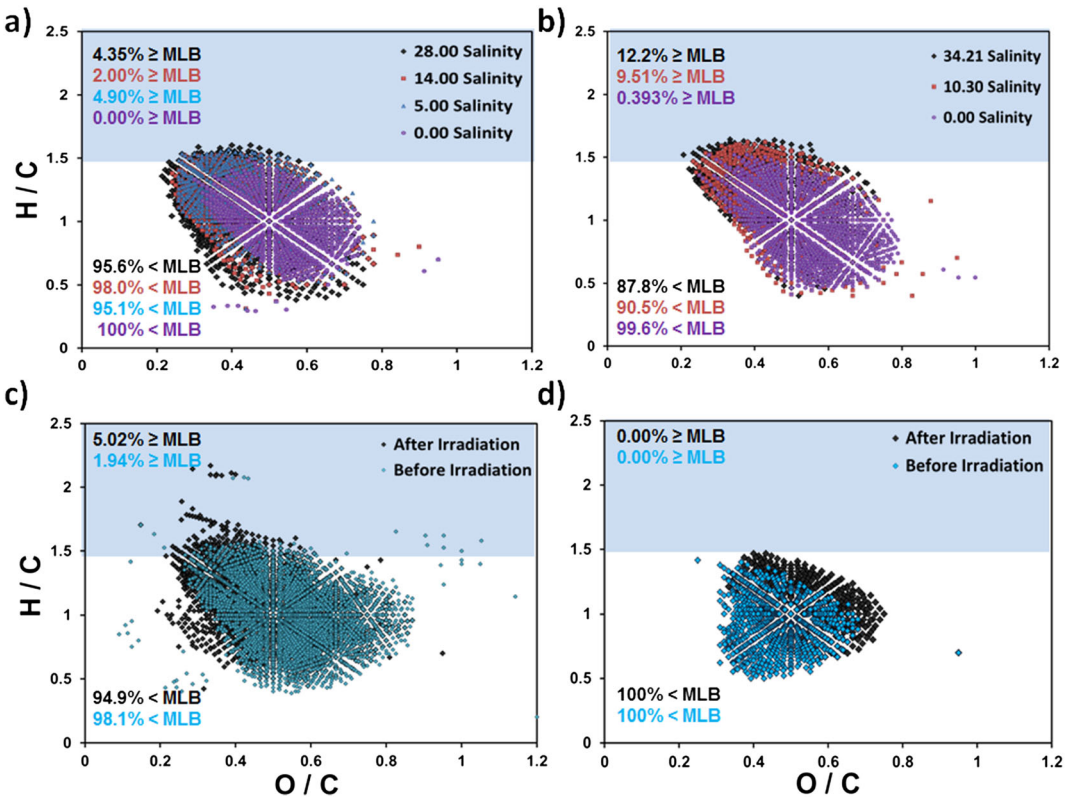

Figure 3. van Krevelen diagrams for organic matter isolated from freshwater and estuarine sources at (a) Freshwater River (New Zealand), ranging from 0.00 to 28.00 in salinity; (b) Doubtful Sound (New Zealand), ranging from 0.00 to 34.21 in salinity; (c) Black River (North Carolina, USA), before and after irradiation; and (d) Cape Fear (North Carolina, USA), before and after irradiation.

To extend these observations further, OM molecular formulae and chemical character of the Gulf of Mexico Brine pool and bottom water samples were compared to the Weddell Sea samples (sea-ice brine and bottom water). Increasing and decreasing trends in MLB_L percentages for each OM molecular species were similarly observed for the Gulf of Mexico brine pool and the Weddell Sea sea-ice brine sample. Even so, Weddell Sea sea-ice brine OM was considerably more labile (28.4%) than the Gulf of Mexico OM brine sample (13.8%) possibly due to the relatively isolated sea-ice environment in which OM is produced.[34,50]

Weddell Sea bottom water is a unique body of water that contributes to the formation of Antarctic Bottom Water (AABW) before circulating around the world. FTICRMS studies have shown that bottom water or "deep sea" OM is

Rapid Communications in Mass Spectrometry

Table 6. Subtropical Convergence (New Zealand) organic matter percent composition and lability for austral summer (January) and winter (August) seasons collected near the coast (STC01), from the center of the convergence (STC04), and in the SubAntarctic surface water (STC08)

	STC01 Summer			STC01 Winter		
Molecular species	Composition (%)	MLB_L (%)	MLB_R (%)	Composition (%)	MLB_L (%)	MLB_R (%)
CHO	65.2	18.2	81.8	88.1	11.2	88.8
$CHOS_1$	33.5	17.8	82.2	10.4	41.1	58.9
$CHON_1$	1.18	0	100	1.50	0	100
$CHON_2$	0.138	0	100	0	0	0
Overall		**17.8**	**82.2**		**14.1**	**85.9**
	STC04 Summer			**STC04 Winter**		
Molecular species	Composition (%)	MLB_L (%)	MLB_R (%)	Composition (%)	MLB_L (%)	MLB_R (%)
CHO	61.2	15.7	84.3	93.5	9.15	90.8
$CHOS_1$	35.6	13.9	86.2	4.82	32.3	67.7
$CHON_1$	3.19	0	100	1.71	0	100
Overall		**14.6**	**85.4**		**10.1**	**89.9**
	STC08 Summer			**STC08 Winter**		
Molecular species	Composition (%)	MLB_L (%)	MLB_R (%)	Composition (%)	MLB_L (%)	MLB_R (%)
CHO	63.3	14.0	86.0	89.4	8.98	91.0
$CHOS_1$	33.6	12.0	88.0	6.48	32.6	67.4
$CHON_1$	3.02	0	100	4.08	0	100
Overall		**12.9**	**87.1**		**10.1**	**89.9**

more recalcitrant in nature, sharing similar chemical character to terrigenous and lignin-like material,[34,51,52] potentially lingering over millennia.[53,54] The Gulf of Mexico and Weddell Sea bottom water samples were predominantly recalcitrant (MLB_R: 92.1% and 91.0%) and displayed strikingly similar chemical composition percentages for all molecular species (Table 4), which may be attributed to the production and/or accumulation of similarly recalcitrant material in both locations influenced by vastly different environmental contributors and the ocean circulation of it globally. Bottom water van Krevelen diagrams for NOM samples from the Gulf of Mexico (Fig. 2(d)) and the Weddell Sea[34] contain molecular data clustered within the same region (H/C: 0.75–1.63 and O/C: 0.2–0.8) describing more recalcitrant, lignin-like material. Based on our understanding of ocean current circulation and the AABW, it is reasonable to speculate that a connection exists between the bodies of water, as the Weddell Sea constituents contributes to the character of the AABW which eventually circulates to the Gulf of Mexico. Therefore, it is possible that predominantly recalcitrant OM, no longer bioavailable to microbes, is globally circulated in deep ocean body waters (>700 m).[52,54] We submit that data generated by FTICRMS with the application of the MLB can provide another metric to measure unique biomolecular tracers worldwide.

Effect of salinity gradients on OM from New Zealand freshwater rivers

Salinity-dependent molecular composition changes in freshwater OM from the Freshwater River on Stewart Island and Doubtful Sound on South Island, New Zealand, were investigated by Gonsior.[55] The Freshwater River OM exhibited greater molecular compositional changes over varying salinities when compared to the Doubtful Sound OM: more aromatic molecular formulae were identified at higher salinities and lignin or lignin-like components remained relatively unchanged.[55] The effect of salinity on OM molecular formulae from the same two aquatic ecosystems for CHO-containing components is presented in Figs. 3(a) and 3(b). Both aquatic ecosystems display molecular data centered within the lignin-like region of the van Krevelen diagrams. Freshwater River OM at higher salinities exhibited either similar or lower degrees of oxygenation over a range of hydrogen saturation (H/C: 0.313–1.6), whereas Doubtful Sound OM exhibited more constituents at higher hydrogen saturation values over a range of O/C ratios (Fig. 3(b)). At zero salinity, both New Zealand freshwater ecosystems exhibited the highest MLB_R (99.6% for Doubtful Sound and 100% for Freshwater River) OM character when compared to all other ecosystems in this study.

The Doubtful Sound contains very high, nearly exclusive terrestrial chromophoric OM character confirmed first by fluorescence spectroscopy.[56] The southwestern slope of the South Island of New Zealand and the northeastern slope of Stewart Island accrue an estimated 400–500 tons of carbon vegetation per hectare with considerable carbon storage values.[57] The lignin-like OM character and recalcitrant nature in both ecosystems could be a result of the higher annual rainfall percentages (>7 m $year^{-1}$ at Doubtful Sound) and the fjord slope mass-wasting soil and vegetation events that deliver terrestrial OM to the soils and surrounding waters.[58] Smith and Bianchi[58] reported $\delta^{13}C$ values for the Doubtful Sound that extend to –28.7‰, characteristic of a more terrestrial, recalcitrant signature, consistent with the FTICRMS results.

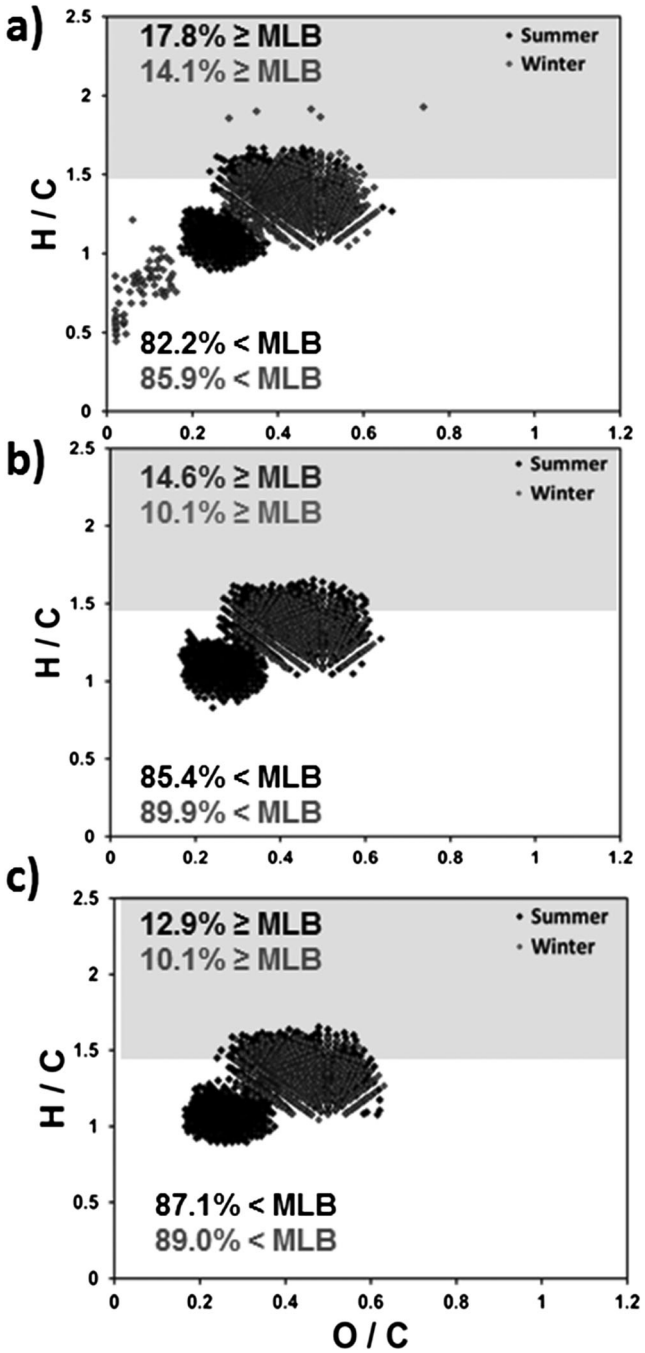

Figure 4. van Krevelen diagrams of Subtropical Convergence (STC) marine organic matter collected in austral summer and winter seasons for (a) coastal waters (STC01) New Zealand; (b) the center of the convergence (STC04); and (c) SubAntarctic surface water (STC08).

The Freshwater River OM shows fluctuating labile character as salinity initially increased, a feature not observed for Doubtful Sound OM; increasing salinity also coincides with increasing labile nature. No differences were observed in that trend for Doubtful Sound OM when considering MLB_{wL} and MLB_{wR}; however, the Freshwater River weighted distributions produced a tighter range of overall labile contributions (MLB_{wL}: 0–1.94% compared to MLB_{wL}: 0–4.90%). Within the MLB_{wL} ranges, considering only CHO molecular species, OM at a salinity of 14.00 was ranked as having the largest labile contribution to the overall OM nature followed by salinities measured at 28.00, 5.00, and zero. Although many variables can affect OM character in these environments, overall, labile nature generally increases with salinity for OM from the Freshwater River and Doubtful Sound.

North Carolina freshwater and estuary-irradiated OM

Solar irradiation effects on OM molecular composition vary with source material and environmental contributions.[25] To capture the qualitative molecular shifts in sunlight-induced, photo-reactive changes in OM from different environments, Black River and adjoining Cape Fear estuary samples were collected, exposed for 21 h to a 1000 W Spectral Energy solar simulator, and analyzed by FTICRMS.[25] As an extension of the reported data from that experiment, Table 5 and Figs. 3 (c) and 3(d) include the $C_cH_hN_nO_oS_s$ and $C_cH_hO_o$ assignment results with MLB fractions for Black River and Cape Fear estuary OM determined by FTICRMS. An increase in Black River OM molecular constituents containing CHO and $CHON_1$, and a decrease in $CHOS_1$, $CHON_1S_1$, and $CHON_2$, were observed after irradiation exposure. Black River OM contained a relatively low percentage of molecular constituents for MLB_L before and after irradiation (1.94% and 5.02%), whereas Cape Fear OM contained no MLB_L. Moreover, the MLB_L percentages increased for CHO, $CHOS_1$, and $CHON_1$, indicating that irradiation may be responsible for the OM transformation to more labile constituents at higher hydrogen saturation values. Figures 3(c) and 3(d) show chemical character overlap for each irradiation comparison, and display the increase in labile nature toward or above the MLB after irradiation. A decrease in oxygenation after irradiation was observed for Black River OM, but not for Cape Fear OM. Cape Fear estuary OM contained only CHO molecular species for MLB_R; however, the irradiated OM contained molecular formulae that extend to higher H/C ratios showing an increase in hydrogen saturation after irradiation (Fig. 3(d)). Taken together, photochemical changes target unsaturated, aromatic, and less oxygenated OM molecular constituents, similar to the results reported in Kujawinski *et al.*,[24] and, although the two environments are very different, a consistent increase in hydrogen saturation in MLB_L or near the MLB was observed after irradiation.

Bioavailability of OM in the Cape Fear River was assessed by weekly experiments of incubated river samples in the dark to monitor organic carbon concentration loss over time.[59] Avery *et al.*[59] reported that the fraction of bioavailable OM (consumed organic constituents) was relatively small (9.0 ± 4.5%), indicating that the Cape Fear River contains mostly recalcitrant OM, not available for biological consumption, and that all bioavailable values calculated for this system fell within the ranges reported for other river studies (1–30%).[59] Furthermore, the Cape Fear River system has been previously characterized as containing extremely high humic content apparent in concentration (~50 mg L^{-1})[60] and fluorescent nature.[25] These results corroborate the FTICRMS findings with the application of the MLB, with low bioavailable carbon constituents detected, highlighting similar results in bioavailability without longer term biological incubations.

Rapid Communications in Mass Spectrometry

Table 7. Northern Minnesota Red Lake II peatland fen and bog porewater organic matter percent composition and lability for samples collected at the surface and at depth

	Bog Deep 250 cm			Bog Surface 17 cm		
Molecular species	Composition (%)	MLB_L (%)	MLB_R (%)	Composition (%)	MLB_L (%)	MLB_R (%)
CHO	92.5	3.37	96.6	91.2	2.07	97.9
$CHOS_1$	0.351	29.4	70.6	0.889	20.0	80.0
$CHON_1$	7.09	0	100	7.86	0	100
$CHON_2$	0.103	0	100	0.036	0	100
Overall		**3.22**	**96.8**		**2.06**	**97.9**
	Fen Deep 250 cm			**Fen Surface 20 cm**		
Molecular species	Composition (%)	MLB_L (%)	MLB_R (%)	Composition (%)	MLB_L (%)	MLB_R (%)
CHO	63.9	4.97	95.0	80.1	3.03	96.9
$CHOS_1$	3.24	0.361	99.6	0.175	62.5	37.5
$CHON_1$	20.9	0	100	14.6	0	100
$CHON_2$	7.90	0	100	4.07	0	100
$CHON_3$	4.11	0	0	0.986	0	0
Overall		**3.18**	**96.8**		**2.54**	**97.4**

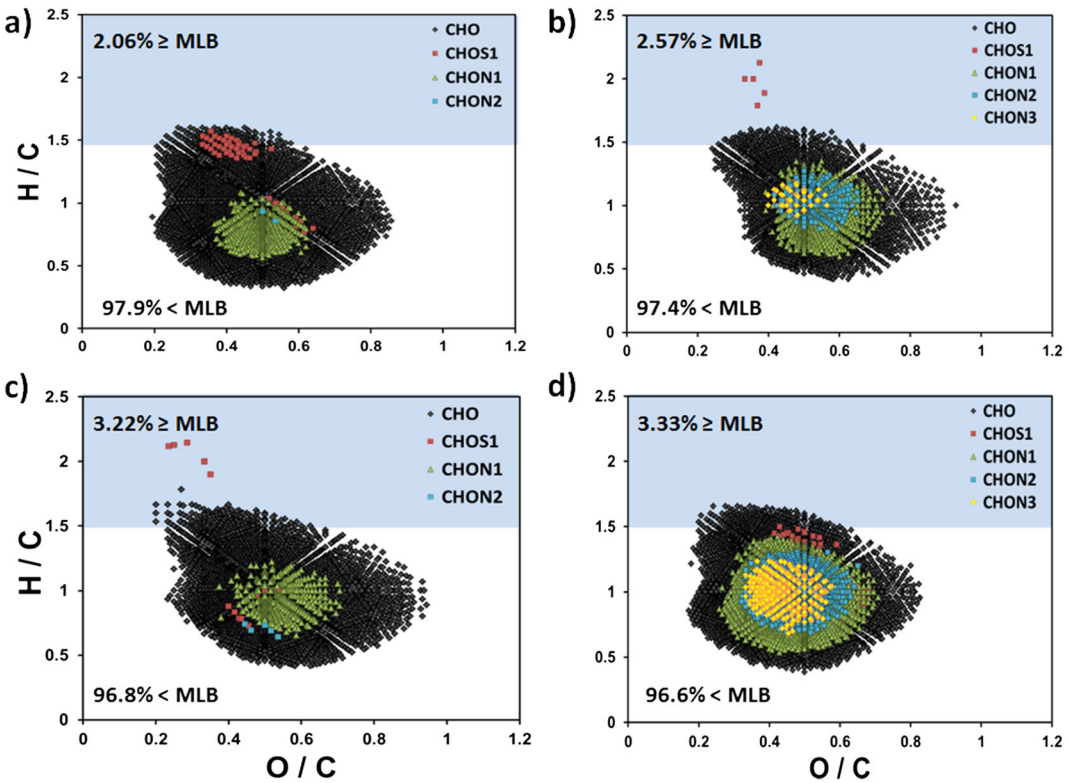

Figure 5. Northern Minnesota Red Lake II peatland porewater organic matter van Krevelen diagrams of (a) surface bog (17 cm); (b) deep bog (250 cm); (c) surface fen (20 cm); and (d) deep fen (250 cm).

Marine OM seasonality shifts from New Zealand ocean waters

The molecular characterization of marine OM considering $C_cH_hN_nO_oS_s$ molecular formula assignments by FTICRMS was determined for six samples of the Subtropical Convergence (STC) east of South Island, New Zealand, by Gonsior and co-workers.[38] Six samples were collected in total, including three different regions of the STC for austral summer and winter seasons: near coast, central STC, and SubAntarctic surface water (STC01, STC04, and STC08).[38] The percentage of MLB_L for all STC marine samples fell between 10.1 and 17.8, with more hydrogen-saturated species and thus labile character than freshwater OM, and more recalcitrant character than microbially derived marine and glacial environments. Summer season OM for each marine STC location was determined to have more S-containing molecular species relative to austral winter, which may reflect

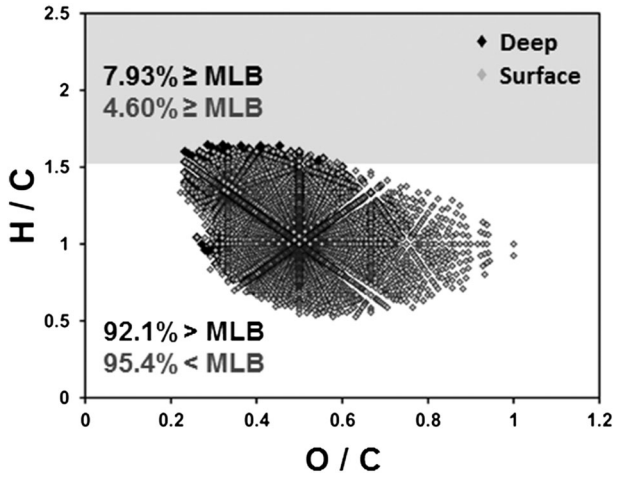

Figure 6. van Krevelen diagram of CHO-containing organic matter from northern Minnesota Lost River surface and deep bog porewaters (20 cm and 250 cm).

seasonal heightened biological activity.[38] A higher percentage of MLB_{wL} was also reported for the $CHOS_1$ molecular species contribution for all STC samples in the summer season. A general increase in CHO-containing OM constituents and decrease in heterogeneous constituents is observed in OM composition for the transition from austral summer to winter seasons (Table 6). Applying the MLB_L reveals that STC OM contained more labile S-containing richness in the austral winter season, though the percent composition of $CHOS_1$ contributions to the overall marine OM composition is higher for austral summer.

Each summer OM sample extends to higher H/C, above the MLB in the protein-like region, ranging from O/C ratios of 0.2–0.6 for $C_cH_hN_nO_oS_s$-containing molecular species collected across the STC (Figs. 4(a)–4(c)). Each van Krevelen diagram shows that most of the molecular data range from H/C 1.0–1.7 and O/C 0.2–0.6, grouped in two distinct clusters: the lower H/C cluster corresponds to $CHOS_1$-containing molecular species. Molecular formulae containing S at higher H/C ratios were suggested to arise from marine biogenic sulfolipids, known for the production of labile organic constituents.[38,61] Satellite imaging near the sample collection dates detected algal blooms throughout the STC transect for both seasons and revealed heightened algal activity in the summer;[38] therefore, more OM molecular species above the MLB was expected for the summer, especially near the coast. This trend is apparent in both Figs. 4(a)–4(c) and Table 6: more labile S-containing species are detected in the summer and can be organized across the oceanic transect by labile nature: STC01 > STC04 > STC08. Overall OM lability decreases with increasing distance from the terrestrial coastline for the summer; however it is less pronounced in the winter.

Northern Minnesota peatland porewater OM

The qualitative differences in chemical character for $C_cH_hO_o$-containing molecular species for GLAP bogs and fens in the Red Lake II system of Northern Minnesota determined by FTICRMS were reported by D'Andrilli and co-workers.[62] The heterogeneous character of $C_cH_hN_nO_oS_s$ species for bog and fen surface and deep samples (Table 7) was also considered, but not entirely reported earlier by D'Andrilli.[37]

The Red Lake II fen is unique compared to other GLAP fens due to its similar *Sphagnum*-woody bog character, also found at Red Lake II bog.[62,63] This fen was produced by the pooling of mineral-rich water adjacent to the raised bog at Red Lake II,[63] creating a poor fen environment. Similar characteristics for bog and fen samples are highlighted for $C_cH_hO_o$ molecular species denoted with (♦) symbols in Figs. 5(a)–5(d). Although the fen and bog samples exhibited relatively low labile nature (MLB_L: 2.06–3.33%) relative to the other environmental NOM samples, they both exhibited more labile richness at the deeper strata, with the surface bog OM having the most recalcitrant nature.

Peatland landforms, such as bogs and fens, are classified based on a variety of environmental factors including: land formation, water chemistry, vegetation, and hydrology,[64,65] all of which in turn affect the OM production, consumption, and accumulation, at each depth within the peat profile, and thus its molecular composition. OM heterogeneous species above and below the MLB for Red Lake II bog and fen are shown in Figs. 5(a)–5(d). All samples show most OM molecular species in MLB_R, displaying similarly recalcitrant chemical nature. Only CHO and $CHOS_1$ groups extend into the more labile region of the diagram at higher H/C ratios for each bog and fen OM sample, possibly a result of the changing environmental conditions and microbial communities within different strata.

The goal of the Red Lake II peatland OM project was to chemically characterize the OM in fens and bogs at varying depths by FTICRMS.[37,62] However, not all fens and bogs exhibit identical chemical character. Therefore, another peatland system (Lost River; LR) was also selected to compare differences in bog-like OM character at various depths with the Red Lake II system (Fig. 6). For the LR bog, the degree of oxygenation and hydrogen saturation is lower for the deeper samples, and the surface sample contains molecular formulae over a broad range of O/C ratios. Comparatively, the LR bog sample at depth shares the same oxygenation trend with the Red Lake II peatland fen.

The general trend in more labile OM for the Red Lake II bog and fen samples at depth was also observed for the LR bog OM. It should be noted that all of the Red Lake II system fen and bog samples grouped together in MLB_L (2.06–3.33%), whereas the LR bog samples had a more extended distribution (4.60–7.93%). As more labile molecular species relate directly to more microbial influence, and the environments are characterized by different OM, we speculate that the variations in labile character in each peatland landform originate from different microbial communities in the GLAP.[66] Thus, the LR bog at deeper strata may house a more favorable environment for carbon turnover by microbes, incorporating OM consumption, transformation, and production, altogether resulting in the highest MLB_L richness value (7.93%) of all the peatland samples.

CONCLUSIONS

FTICRMS data are extremely useful for the molecular analysis of NOM character, source material, and evolution. The van Krevelen diagram remains the most effective visual method to define NOM composition as a function of different chemical classes and operative reaction pathways. The MLB

Rapid Communications in Mass Spectrometry

extends the van Krevelen analysis to include NOM lability. In this study, 35 samples, spanning molecular composition analysis for the same FTICRMS instrument over the course of a decade, were compared in terms of NOM chemical composition and lability. The MLB is a dividing threshold that differentiates NOM data into more and less labile molecular groups based on its degree of hydrogen saturation and chemical character. For the MLB application to FTICRMS data, an estimation of NOM ecosystem lability is possible from a single mass spectrum when other biological data are not available.

The MLB molecular richness and MLB_w diversity calculations generally ranked the ecosystem NOM from most to least labile as glacial > marine > freshwater. Notably, the ecosystems that represent the most purely autochthonous, microbially derived OM, hypothesized to be the most labile OM source, all were reported to have the highest contributions of more hydrogen-saturated species and labile material distinguished by the MLB and MLB_w. Also, none of those environments have MLB-based labile percentages of 100%, reinforcing the notion that autochthonous OM can also contain other types of chemical character that group in less labile regions of the van Krevelen diagram. With the MLB and MLB_w, it is possible to distinguish more and less labile OM and their contributions to the overall ecosystem from different environments. That capability is especially important because environments are influenced differently by allochthonous and/or autochthonous contributions, including microbial processes. Even when considering ecosystem complexity, the MLB information can provide insight about physical, chemical, and biological processes affecting OM across a diverse array of ecosystems from around the world.

Acknowledgements

We thank all participants who supported and promoted the advancements of NOM FTICRMS characterization research at the National High Magnetic Field Laboratory in Tallahassee, Florida, within the last ten years, specifically Y.-P. Chin, J. P. Chanton, W. J. Cooper, T. Dittmar, P. H. Glaser, M. Huettel, J. Kostka, B. P. Koch, D. M. McKnight, B. M. Peake, D. I. Siegel, and their respective sample collection teams in Antarctica (including H. J. Smith), New Zealand, and the USA. Also, we thank L. Chipman, and M. Gonsior, for their contributions to the scientific community that were referenced for this comparative work. This work would not have been possible without the help of D. C. Podgorski and B. Ruddy, and also the efforts of the Ion Cyclotron Resonance Facility Staff at the NHMFL that maintain the optimal performance of the 9.4 tesla FTICR mass spectrometer. In addition, we thank J. R. Junker for his intellectual creativity and suggestions to improve this work. Support was provided by NSF Division of Materials Research through DMR-11-57490 and the State of Florida.

REFERENCES

[1] J. P. Hassett, M. A. Anderson. Effects of dissolved organic-matter on adsorption of hydrophobic organic-compounds by river-borne and sewage-borne particles. *Water Res.* **1982**, *16*, 681.

[2] P. H. Santaschi, J. J. Lenhart, B. D. Honeyman. Heterogeneous processes affecting trace contaminant distribution in estuaries: The role of natural organic matter. *Mar. Chem.* **1997**, *58*, 99.

[3] R. Benner, J. D. Pakulski, M. Mccarthy, J. I. Hedges, P. G. Hatcher. Bulk chemical characteristics of dissolved organic-matter in the ocean. *Science* **1992**, *255*, 1561.

[4] J. I. Hedges, G. Eglinton, P. G. Hatcher, D. L. Kirchman, C. Arnosti, S. Derenne, R. P. Evershed, I. Kogel-Knabner, J. W. de Leeuw, R. Littke, W. Michaelis, J. Rullkotter. The molecularly-uncharacterized component of nonliving organic matter in natural environments. *Org. Geochem.* **2000**, *31*, 945.

[5] A. D. Redman, D. L. Macalady, D. Ahmann. Natural organic matter affects arsenic speciation and sorption onto hematite. *Environ. Sci. Technol.* **2002**, *36*, 2889.

[6] W. V. Sobczak, J. E. Cloern, A. D. Jassby, A. B. Muller-Solger. Bioavailability of organic matter in a highly disturbed estuary: The role of detrital and algal resources. *Proc. Natl. Acad. Sci. USA* **2002**, *99*, 8101.

[7] B. C. Crump, G. W. Kling, M. Bahr, J. E. Hobbie. Bacterioplankton community shifts in an arctic lake correlate with seasonal changes in organic matter source *Appl. Environ. Microbiol.* **2003**, *69*, 2253.

[8] D. A. Hansell, C. A. Carlson. Marine dissolved organic matter and the carbon cycle. *Oceanography* **2001**, *14*, 41.

[9] S. Kim, R. W. Kramer, P. G. Hatcher. Graphical method for analysis of ultrahigh-resolution broadband mass spectra of natural organic matter, the van Krevelen diagram. *Anal. Chem.* **2003**, *75*, 5336.

[10] K. Mopper, A. Stubbins, J. D. Ritchie, H. M. Bialk, P. G. Hatcher. Advanced instrumental approaches for characterization of marine dissolved organic matter: Extraction techniques, mass spectrometry, and nuclear magnetic resonance spectroscopy. *Chem. Rev.* **2007**, *107*, 419.

[11] R. A. Berner. Biogeochemical cycles of carbon and sulfur and their effect on atmospheric oxygen over Phanerozoic time. *Global Planet. Change* **1989**, *75*, 97.

[12] T. J. Battin, L. A. Kaplan, S. Findlay, C. S. Hopkinson, E. Marti, A. I. Packman, J. D. Newbold, F. Sabater. Biophysical controls on organic carbon fluxes in fluvial networks. *Nat. Geosci.* **2008**, *1*, 95.

[13] B. P. Koch, T. Dittmar. From mass to structure: An aromaticity index for high-resolution mass data of natural organic matter. *Rapid Commun. Mass Spectrom.* **2006**, *20*, 926.

[14] T. Santl-Temkiv, K. Finster, T. Dittmar, B. M. Hansen, R. Thyrhaug, N. W. Nielsen, U. G. Karlson. Hailstones: A window into the microbial and chemical inventory of a storm cloud. *PLoS One* **2013**, *8*, e53550.

[15] A. M. Kellerman, T. Dittmar, D. N. Kothawala, L. J. Tranvik. Chemodiversity of dissolved organic matter in lakes driven by climate and hydrology. *Nat. Commun.* **2014**, 5.

[16] A. G. Marshall, C. L. Hendrickson, G. S. Jackson. Fourier transform ion cyclotron resonance mass spectrometry: A primer. *Mass Spectrom. Rev.* **1998**, *17*, 1.

[17] D. C. Podgorski, R. Hamdan, A. M. McKenna, L. Nyadong, R. P. Rodgers, A. G. Marshall, W. T. Cooper. Characterization of pyrogenic black carbon by desorption atmospheric pressure photoionization Fourier transform ion cyclotron resonance mass spectrometry. *Anal. Chem.* **2012**, *84*, 1281.

[18] J. D'Andrilli, C. M. Foreman, A. G. Marshall, D. M. McKnight. Characterization of IHSS Pony Lake fulvic acid dissolved organic matter by electrospray ionization Fourier transform ion cyclotron resonance mass spectrometry and fluorescence spectroscopy. *Org. Geochem.* **2013**, *65*, 19.

[19] E. C. Minor, M. M. Swenson, B. M. Mattson, A. R. Oyler. Structural characterization of dissolved organic matter: A review of current techniques for isolation and analysis. *Environ. Sci. Processes Impacts* **2014**, *16*, 2064.
[20] A. C. Stenson, A. G. Marshall, W. T. Cooper. Exact masses and chemical formulas of individual Suwannee River fulvic acids from ultrahigh resolution electrospray ionization Fourier transform ion cyclotron resonance mass spectra. *Anal. Chem.* **2003**, *75*, 1275.
[21] A. M. Grannas, W. C. Hockaday, P. G. Hatcher, L. G. Thompson, E. Mosley-Thompson. New revelations on the nature of organic matter in ice cores. *J. Geophys. Res. – Atmospheres* **2006**, 111.
[22] M. P. Bhatia, S. B. Das, K. Longnecker, M. A. Charette, E. B. Kujawinski. Molecular characterization of dissolved organic matter associated with the Greenland ice sheet. *Geochim. Cosmochim. Acta* **2010**, *74*, 3768.
[23] L. Chipman, D. Podgorski, S. Green, J. Kostka, W. Cooper, M. Huettel. Decomposition of plankton-derived dissolved organic matter in permeable coastal sediments. *Limnol. Oceanogr.* **2010**, *55*, 857.
[24] E. B. Kujawinski, R. Del Vecchio, N. V. Blough, G. C. Klein, A. G. Marshall. Probing molecular-level transformations of dissolved organic matter: Insights on photochemical degradation and protozoan modification of DOM from electrospray ionization Fourier transform ion cyclotron resonance mass spectrometry. *Mar. Chem.* **2004**, *92*, 23.
[25] M. Gonsior, B. M. Peake, W. T. Cooper, D. Podgorski, J. D'Andrilli, W. J. Cooper. Photochemically induced changes in dissolved organic matter identified by ultrahigh resolution Fourier transform ion cyclotron resonance mass spectrometry. *Environ. Sci. Technol.* **2009**, *43*, 698.
[26] T. Dittmar, B. Koch, N. Hertkorn, G. Kattner. A simple and efficient method for the solid-phase extraction of dissolved organic matter (SPE-DOM) from seawater. *Limnol. Oceanogr. – Methods* **2008**, *6*, 230.
[27] M. R. Emmett, F. M. White, C. L. Hendrickson, S. D. H. Shi, A. G. Marshall. Application of micro-electrospray liquid chromatography techniques to FT-ICR MS to enable high-sensitivity biological analysis. *J. Am. Soc. Mass Spectrom.* **1998**, *9*, 333.
[28] G. T. Blakney, C. L. Hendrickson, A. G. Marshall. Predator data station: A fast data acquisition system for advanced FT-ICR MS experiments. *Int. J. Mass Spectrom.* **2011**, *306*, 246.
[29] N. K. Kaiser, J. P. Quinn, G. T. Blakney, C. L. Hendrickson, A. G. Marshall. A novel 9.4 Tesla FTICR mass spectrometer with improved sensitivity, mass resolution, and mass range. *J. Am. Soc. Mass Spectrom.* **2011**, *22*, 1343.
[30] A. G. Marshall, F. R. Verdun. *Fourier Transforms in NMR, Optical, and Mass Spectrometry: A User's Handbook*. Elsevier, Amsterdam, **1990**.
[31] P. A. Limbach, L. Schweikhard, K. A. Cowen, M. T. Mcdermott, A. G. Marshall, J. V. Coe. Observation of the doubly charged, gas-phase fullerene anions C_{60}^{2-} and C_{70}^{2-}. *J. Am. Soc. Mass Spectrom.* **1991**, *113*, 6795.
[32] T. L. Brown, J. A. Rice. Effect of experimental parameters on the ESI FT-ICR mass spectrum of fulvic acid. *Anal. Chem.* **2000**, *72*, 384.
[33] E. B. Kujawinski, P. G. Hatcher, M. A. Freitas. High-resolution Fourier transform ion cyclotron resonance mass spectrometry of humic and fulvic acids: Improvements and comparisons. *Anal. Chem.* **2002**, *74*, 413.
[34] J. D'Andrilli, T. Dittmar, B. P. Koch, J. M. Purcell, A. G. Marshall, W. T. Cooper. Comprehensive characterization of marine dissolved organic matter by Fourier transform ion cyclotron resonance mass spectrometry with electrospray and atmospheric pressure photoionization. *Rapid Commun. Mass Spectrom.* **2010**, *24*, 643.
[35] J. D. Mao, R. M. Cory, D. M. McKnight, K. Schmidt-Rohr. Characterization of a nitrogen-rich fulvic acid and its precursor algae from solid state NMR. *Org. Geochem.* **2007**, *38*, 1277.
[36] X. W. Fang, J. D. Mao, R. M. Cory, D. M. McKnight, K. Schmidt-Rohr. ^{15}N and $^{13}C\{^{14}N\}$ NMR investigation of the major nitrogen-containing segment in an aquatic fulvic acid: Evidence for a hydantoin derivative. *Magnetic Resonance Chem.* **2011**, *49*, 775.
[37] J. D'Andrilli. *Molecular characterization of marine and terrestrial dissolved organic matter using ultrahigh resolution mass spectrometry.* Florida State University, Tallahassee, Florida, **2009**.
[38] M. Gonsior, B. M. Peake, W. T. Cooper, D. C. Podgorski, J. D'Andrilli, T. Dittmar, W. J. Cooper. Characterization of dissolved organic matter across the Subtropical Convergence off the South Island, New Zealand. *Mar. Chem.* **2011**, *123*, 99.
[39] E. M. Perdue, J. D. Ritchie, in *Treatise on Geochemistry*, (Ed: H. D. H. K. Turekian), Pergamon Press, Oxford, **2003**, p. 273.
[40] J. Shapiro. Chemical and biological studies on the yellow organic acids of lake water. *Limnol. Oceanogr.* **1957**, *2*, 161.
[41] D. M. Osborne, D. C. Podgorski, D. A. Bronk, Q. Roberts, R. E. Sipler, D. Austin, J. S. Bays, W. T. Cooper. Molecular-level characterization of reactive and refractory dissolved natural organic nitrogen compounds by atmospheric pressure photoionization coupled to Fourier transform ion cyclotron resonance mass spectrometry. *Rapid Commun. Mass Spectrom.* **2013**, *27*, 851.
[42] W. Seiler, P. J. Crutzen. Estimates of gross and net fluxes of carbon between the biosphere and the atmosphere from biomass burning. *Clim. Change* **1980**, *2*, 207.
[43] E. W. Behrens. Geology of a Continental-Slope Oil Seep, Northern Gulf of Mexico. *Aapg Bulletin – American Association of Petroleum Geologists* **1988**, *72*, 105.
[44] M. C. Kennicutt, J. M. Brooks, G. J. Denoux. Leakage of deep, reservoired petroleum to the near-surface on the Gulf of Mexico Continental-Slope. *Mar. Chem.* **1988**, *24*, 39.
[45] P. Aharon. Geology and biology of modern and ancient submarine hydrocarbon seeps and vents – an introduction. *Geo-Marine Lett.* **1994**, *14*, 69.
[46] B. Orcutt, A. Boetius, M. Elvert, V. Samarkin, S. B. Joye. Molecular biogeochemistry of sulfate reduction, methanogenesis and the anaerobic oxidation of methane at Gulf of Mexico cold seeps. *Geochim. Cosmochim. Acta* **2005**, *69*, 4267.
[47] I. R. MacDonald, W. W. Sager, M. B. Peccini. Gas hydrate and chemosynthetic biota in mounded bathymetry at mid-slope hydrocarbon seeps: Northern Gulf of Mexico. *Mar. Geol.* **2003**, *198*, 133.
[48] S. M. De Beukelaer, I. R. MacDonald, N. L. Guinnasso Jr., J. A. Murray. Distinct side-scan sonar, RADARSAT SAR, and acoustic profiler signatures of gas and oil seeps on the Gulf of Mexico slope. *Geo-Marine Lett.* **2003**, *23*, 177.
[49] W. W. Sager, I. R. MacDonald, R. S. Hou. Geophysical signatures of mud mounds at hydrocarbon seeps on the Louisiana continental slope, northern Gulf of Mexico. *Mar. Geol.* **2003**, *198*, 97.
[50] G. S. Dieckmann, M. A. Lange, S. F. Ackley, J. C. Jennings. The nutrient status in sea ice of the Weddell Sea during winter – Effects of sea ice texture and algae. *Polar Biol.* **1991**, *11*, 449.
[51] T. Dittmar, G. Kattner. The biogeochemistry of the river and shelf ecosystem of the Arctic Ocean: A review. *Mar. Chem.* **2003**, *83*, 103.
[52] B. P. Koch, M. R. Witt, R. Engbrodt, T. Dittmar, G. Kattner. Molecular formulae of marine and terrigenous dissolved organic matter detected by electrospray ionization Fourier transform ion cyclotron resonance mass spectrometry. *Geochim. Cosmochim. Acta* **2005**, *69*, 3299.

[53] D. A. Hansell, C. A. Carlson, D. J. Repeta, R. Schlitzer. Dissolved organic matter in the ocean: A controversy stimulates new insights. *Oceanography* **2009**, *22*, 202.
[54] N. Jiao, G. J. Herndl, D. A. Hansell, R. Benner, G. Kattner, S. W. Wilhelm, D. L. Kirchman, M. G. Weinbauer, T. Luo, F. Chen, F. Azam. Microbial production of recalcitrant dissolved organic matter: Long-term carbon storage in the global ocean. *Nat. Rev. Micro* **2010**, *8*, 593.
[55] M. Gonsior. Dissolved organic matter in New Zealand natural waters. University of Otago, Dunedin, New Zealand, **2008**.
[56] M. Gonsior, B. Peake, W. Cooper, R. Jaffe, H. Young, A. Kahn, P. Kowalczuk. Spectral characterization of chromophoric dissolved organic matter (CDOM) in a fjord (Doubtful Sound, New Zealand). *Aquatic Sci.* **2008**, *70*, 397.
[57] K. R. Tate, D. J. Giltrap, J. J. Claydon, P. F. Newsome, I. A. E. Atkinson, M. D. Taylor, R. Lee. Organic carbon stocks in New Zealand's terrestrial ecosystems. *J. Royal Soc. New Zealand* **1997**, *27*, 315.
[58] R. W. Smith, T. S. Bianchi, C. Savage. Comparison of lignin phenols and branched/isoprenoid tetraethers (BIT index) as indices of terrestrial organic matter in Doubtful Sound, Fiordland, New Zealand. *Org. Geochem.* **2010**, *41*, 281.
[59] G. B. Avery, J. D. Willey, R. J. Kieber, G. C. Shank, R. F. Whitehead. Lux and bioavailability of Cape Fear River and rainwater dissolved organic carbon to Long Bay, southeastern United States. *Global Biogeochem. Cycles* **2003**, 17.
[60] R. J. Kieber, A. Li, P. J. Seaton. Production of nitrite from the photodegradation of dissolved organic matter in natural waters. *Environ. Sci. Technol.* **1999**, *33*, 993.
[61] A. A. Benson, H. Daniel, R. Wiser. A sulfolipid in plants. *Proc. Natl. Acad. Sci. USA* **1959**, *45*, 1582.
[62] J. D'Andrilli, J. P. Chanton, P. H. Glaser, W. T. Cooper. Characterization of dissolved organic matter in northern peatland soil porewaters by ultra high resolution mass spectrometry. *Org. Geochem.* **2010**, *41*, 791.
[63] P. H. Glaser, G. A. Wheeler, E. Gorham, H. E. Wright. The patterned mires of the Red Lake Peatland, Northern Minnesota – Vegetation, water chemistry and landforms. *J. Ecol.* **1981**, *69*, 575.
[64] H. Sjors. Myrvegetation: Bergaslagen. *Acta Phytogeografica Suecica* **1948**, *21*, 299.
[65] H. Sjors. Bogs and fens on Attawapiskat River, Northern Ontario. *Bull. National Museum of Canada* **1963**, *186*, 45.
[66] X. Lin, S. Green, M. M. Tfaily, O. Prakash, K. T. Konstantinidis, J. E. Corbett, J. P. Chanton, W. T. Cooper, J. E. Kostka. Microbial community structure and activity linked to contrasting biogeochemical gradients in bog and fen environments of the Glacial Lake Agassiz peatland. *Appl. Environ. Microbiol.* **2012**, *78*, 7023.
[67] L. Chipman. Oxygen and dissolved organic carbon dynamics in permeable coastal sediments. Florida State University, Tallahassee, Florida, **2011**.